

On the Electronic Impact of Abnormal C4-Bonding in N-Heterocyclic Carbene Complexes

Marion Heckenroth,^[a] Antonia Neels,^[b] Michael G. Garnier,^[c] Philipp Aebi,^[c]
Andreas W. Ehlers,^[d] and Martin Albrecht^{*[a]}

Abstract: Sterically similar palladium dicarbene complexes have been synthesized that comprise permethylated dicarbene ligands which bind the metal center either in a normal coordination mode via C2 or abnormally via C4. Due to the strong structural analogy of the complexes, differences in reactivity patterns may be attributed to the distinct electronic impact of normal versus abnormal carbene bonding, while stereoelectronic effects are negligible. Unique reactivity patterns have

been identified for the abnormal carbene complexes, specifically upon reaction with Lewis acids and in oxidative addition-reductive elimination sequences. These reactivities as well as analytical investigations using X-ray diffraction and X-ray photoelectron spectroscopy

indicate that the C4 bonding mode increases the electron density at the metal center substantially, classifying such C4-bound carbene ligands amongst the most basic neutral donors known thus far. A direct application of this enhanced electron density at the metal center is demonstrated by the catalytic H₂ activation with abnormal carbene complexes under mild conditions, leading to a catalytic process for the hydrogenation of olefins.

Keywords: coordination modes • electronic tuning • metal nucleophilicity • N-heterocyclic carbene ligands • palladium

Introduction

In the last few years, *N*-heterocyclic carbenes (NHCs) have emerged as versatile ligands in organometallic chemistry and homogeneous catalysis.^[1] Their successful application has been attributed generally to the covalent M–C bond character and to the stronger donor properties as compared to other neutral donor ligands such as phosphines. Recently,

abnormal C4-bonding of NHCs, discovered few years ago,^[2] has been suggested to further increase the donor properties of this class of ligands substantially.^[3] As a consequence, enhanced reactivity of C4-bound carbene metal complexes has been observed for stoichiometric and catalytic bond activation processes.^[3b,4] Stronger ligand donation may be rationalized by the presence of only one heteroatom adjacent to the carbene carbon.^[5] While the absence of a second heteroatom reduces the stability of the free carbene,^[6] the σ -donor ability is increased due to the lower inductive influence of the nitrogen atoms. Furthermore, in abnormal carbenes, that is, in carbenes that do not possess a neutral M=C carbene resonance structure,^[7] the charges in the zwitterionic resonance forms are typically better separated than in normal NHCs, where the positive and negative charge are both localized within the amidinium NCN fragment.^[8] Better charge separation is thought to reinforce the anionic character of the metal-bound carbon and hence to enhance its donor ability. An increased relevance of the zwitterionic resonance form as ground state has been postulated also for related pyrazolylidene complexes.^[9,10]

Owing to the higher acidity of the proton bound to C2 as compared to C4,^[11] abnormal NHC bonding is most often^[12] promoted by protection of the C2 position and subsequent metallation at C4 (or C5) via direct C–H bond activa-

[a] M. Heckenroth, Prof. Dr. M. Albrecht
Department of Chemistry
University of Fribourg
Chemin du Musée 9, 1700 Fribourg (Switzerland)
Fax: (+41) 263-009-738
E-mail: martin.albrecht@unifr.ch

[b] Dr. A. Neels
XRD Application Lab, CSEM
Rue Jaquet Droz 1, 2000 Neuchâtel (Switzerland)

[c] Dr. M. G. Garnier, Prof. Dr. P. Aebi
Physics Institute, University of Neuchâtel
Rue A.-L. Breguet 1, 2000 Neuchâtel (Switzerland)

[d] Dr. A. W. Ehlers
Scheikundig Laboratorium, Vrije Universiteit van Amsterdam
De Boelelaan 1083, 1081 HV Amsterdam (The Netherlands)

Supporting information for this article is available on the WWW under <http://dx.doi.org/10.1002/chem.200900249>.

tion.^[8,13] In part as a consequence of this approach, the C5 carbon in the *ortho* position of C4-metallated imidazolylienes generally features a proton substituent only.^[14] In contrast, normal NHCs possess alkyl or aryl substituents on both *ortho*-positions, that is, on the heteroatoms.^[15] When comparing the two carbene bonding modes, hence, stereo-electronic effects often interfere with electronic alterations due to different substitution of the *ortho* positions.

To unambiguously evaluate the electronic impact of normal and abnormal NHCs we have devised the sterically strongly related dicarbene ligands shown in Figure 1, com-

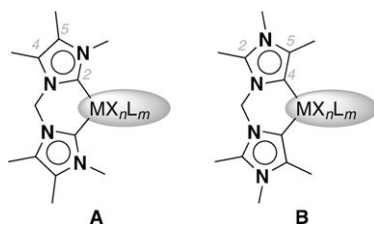
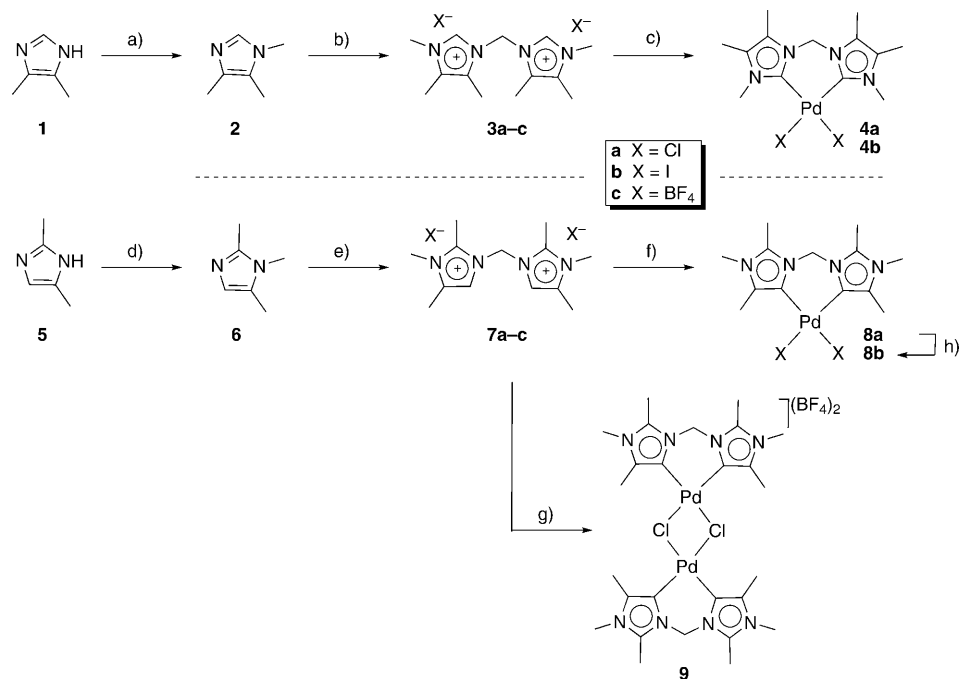


Figure 1. Metal complexes comprising sterically identical cis-chelating dicarbene ligands for investigating the electronic impact of C2-binding (**A**) as opposed to C4-binding of the metal center (**B**).

prising a completely methylated periphery of the heterocycles. Considering that the N–CH₃ and the C–CH₃ bond lengths are equal within standard deviations (1.485(9) Å and 1.503(11) Å, respectively),^[16] the two dicarbene ligands in complexes **A** and **B** impose an identical steric environment around the metal center, yet they feature normal C2- and abnormal C4-bonding,^[17] respectively. The *cis*-chelating binding mode of these dicarbene ligands restricts the number of available coordination sites at the metal center, in particular when bound to square-planar d⁸ platinum group metals. In addition, such chelation prevents any isomerization of the carbene ligands into a mutual *trans* orientation, which would abrogate most of the expected electronic effects such as the *trans* influence and, catalytically presumably more relevant, the *trans* effect. Here we report on the synthesis, the reactivity differences, and the remarkably changed catalytic activity of palladium(II) complexes comprising such sterically strongly related dicarbene ligands and provide unambiguous evidence for the unique electronic impact of C4-bound imidazolylienes.

Results and Discussion

Synthesis of complexes: The potentially C2-binding permethylated dicarbene ligand precursor was prepared starting from the known^[18] 4,5-dimethylimidazole **1** (Scheme 1). *N*-alkylation with MeI gave the 1,4,5-trimethylimidazole **2**, which was subsequently treated with CH₂I₂ or CH₂Cl₂ to yield the diimidazolium salts **3a** and **3b**, respectively. Both products can be converted into the corresponding BF₄[−] salt **3c** by halide abstraction with two molar equivalents of AgBF₄. Metallation of **3a** with Pd(OAc)₂ in DMSO at elevated temperature according to established procedures^[19] afforded the expected cyclopalladated dicarbene complex **4a** in high yields. Likewise, complex **4b** was obtained from the diimidazolium diiodide **3b** and Pd(OAc)₂ by thermally induced cyclometallation. The chloride complex **4a** was also available from the imidazolium salt **3c** with Pd(OAc)₂ in the presence of excess KCl. The ¹H NMR spectra of complexes **4a** and **4b** are similar and reveal significant changes when compared with those of the imidazolium ligand precursors. In particular, the resonance due to the bridging methylene group is shifted upfield by nearly 1 ppm and appears as an AB doublet centered at δ_H = 6.04 and 5.88 ppm in **4a** and at δ_H = 6.02 and 5.87 ppm in **4b**. The inequivalence of these CH₂ protons indicates a rigid boat-type configuration and a restricted flexibility about the Pd–C bond. Such steric constraints may arise due to the repulsive interactions of methyl groups in the C4/C5 position and the CH₂ protons, which disfavor an inversion of the metallacycle. In complexes having protonated C4 and C5 nuclei, metallacycle inversion



Scheme 1. a) Reagents and conditions: a) MeI, DMSO 65°C, 18 h; b) CH₂Cl₂, 150°C μwave, 0.5 h, or CH₂I₂, toluene 110°C, 14 h; c) Pd(OAc)₂ (for **3c**: Pd(OAc)₂, KCl), DMSO 120°C, 3 h; d) Ac₂O, benzene 80°C, 2 h, then MeI, 140°C, 16 h; e) CH₂Cl₂, μwave 150°C, 0.5 h, or CH₂I₂, neat 140°C, 16 h; f) for **7a** Pd(OAc)₂, DMSO 120°C, 3 h; g) for **7c** Pd(OAc)₂, KCl, DMSO 120°C, 3 h; h) AgBF₄, MeCN, 18 h, then Bu₄NI, MeCN 1 h.

is fast at room temperature.^[19] In the ¹³C NMR spectrum the signal for the metal-bound carbon appears at $\delta=155.8$ and 161.1 ppm for **4a** and **4b**, respectively, a frequency that is typical for related C2-bound dicarbene palladium complexes.^[19,20] The chemical shift difference between **4a** and **4b** may be, in part, due to weaker bonding of iodide in **4b**, perhaps as a consequence of steric congestion (cf. X-ray results below).

The permethylated diimidazolium salt precursor for the analogous C4-bound dicarbene complexes was synthesized from commercially available 2,4-dimethylimidazole (**5**) by regioselective alkylation (Scheme 1). For this purpose, the sterically less shielded nitrogen nucleus was protected in situ with acetic anhydride prior to *N*-alkylation using MeI. Subsequent cleavage of the acyl group under basic conditions afforded the 1,2,5-trimethylimidazole **6** in moderate yield. NOESY experiments confirmed the formation of the desired isomer. For example saturation of the signal at $\delta=3.66$ ppm, attributed to the N-bound CH₃ group, induced a positive Overhauser effect for both methyl signals at $\delta=2.76$ (C2-CH₃) and $\delta=2.26$ ppm (C5-CH₃), but did not affect the C4-bound proton. Conversely, the signal at $\delta=2.26$ ppm revealed a correlation to the C4-bound proton and to the N-bound methyl group at $\delta=3.66$ ppm. Notably, direct alkylation of **5** with MeI gave a mixture of 1,2,5- and 1,2,4-trimethylimidazoles. All our attempts to separate the desired isomers by column chromatography or by fractional crystallization of the corresponding imidazolium salt were unsuccessful. Subsequent quaternization of 1,2,5-trimethylimidazole (**6**) with CH₂Cl₂ or CH₂I₂ yielded the diimidazolium salts **7a** and **7b**, respectively, and after anion exchange using AgBF₄, the halide-free analogue **7c**. Metallation of **7a** with Pd(OAc)₂ in DMSO, under conditions identical to those used for the preparation of the C2-bound dicarbene complexes yielded the abnormal dicarbene complex **8a** (Scheme 1). Successful palladation was indicated by ¹H NMR spectroscopy due to the disappearance of the C4-bound proton and a splitting of the CH₂ group into an AB doublet located at $\delta_{\text{H}}=6.33$ and 5.93 ppm ($^2J_{\text{HH}}=12.9$ Hz). The analogous iodide complex **8b** was obtained by successive addition of first AgBF₄ and then Bu₄NI to **8a** in MeCN solution. In solution, complexes **8a** and **8b** feature diastereotopic methyl groups at the C5 and the C5' carbon, as revealed by two distinct singlets in the ¹H and ¹³C spectra, respectively. Such diastereotopicity may arise from solvolysis of one Pd–X bond.^[21]

Remarkably, direct palladation of the iodide **7b** failed under similar reaction conditions. Higher temperatures, longer reaction times, or addition of an external base such as NaOAc or Et₃N did not afford the expected palladium complex, and instead only the starting ligand was recovered. Possibly, the palladate [Pd(OAc)₂I]₂²⁻, which is expected to be generated from **7b** and Pd(OAc)₂,^[20a] is not nucleophilic enough to activate the diimidazolium C4–H bond of **7**.^[22] In contrast, activation of this bond is obviously successful with the more electron-rich precursor [Pd(OAc)₂Cl]₂²⁻, formed from **7a** and Pd(OAc)₂. Palladation of the imidazolium salt

7c comprising BF₄⁻ anions in the presence of KCl afforded, unlike its potentially C2-bonding analogue **3c**, the dimeric palladium complex **9** in good yields. The ¹H NMR spectrum of monomeric **8a** and dimetallic **9** are highly similar, and unambiguous confirmation of the dimeric nature of **9** required single crystal structure determinations and elemental analyses. Notably, depending on the solvent used for the crystallization pseudo-polymorphs are formed. From DMSO, the compound crystallized as colorless blocks in the centrosymmetric triclinic space group *P* $\bar{1}$ with three molecules of DMSO. Crystals obtained from MeCN/Et₂O mixtures were yellow needles and monoclinic (*P*2₁/*n*), and they contained half a molecule of H₂O per asymmetric unit. In both pseudo-polymorphs, the palladium complexes are virtually identical and bond lengths and angles do not differ significantly.^[23] The molecular structure of one of the polymorphous complexes of **9** is shown in Figure 2 and reveals a di-

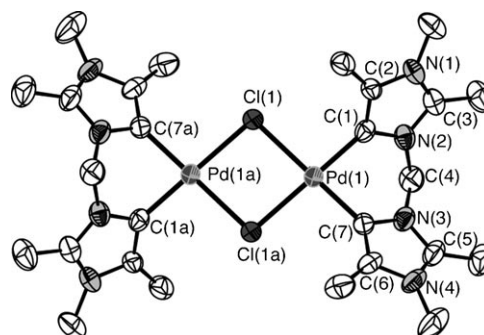


Figure 2. Molecular structure of complex **9** (ORTEP representation, 50% probability level, hydrogen atoms, non-coordinating BF₄⁻ anions and the co-crystallized DMSO molecules omitted for clarity). Selected bond lengths [Å]: Pd(1)–C(1) 1.977(7), Pd(1)–C(7) 1.978(7), Pd(1)–Cl(1) 2.3943(18), Pd(1)–Cl(1a) 2.400(2), Pd(1)–Pd(1a) 3.5395(8); selected bond angles [°]: C(1)–Pd(1)–C(7) 85.0(3), Cl(1)–Pd(1)–Cl(1a) 84.84(7). The pertinent bond lengths and angles in the second polymorph are statistically identical.

cationic palladium dimer bridged by two chloride ligands. The two palladium nuclei are crystallographically equivalent and are located at the center of a slightly distorted square plane. The Pd···Pd distance is $3.54(1)$ Å and hence longer than the sum of the van der Waals radii (3.30 Å), thus suggesting the absence of intermetallic interactions. The Pd–C bond lengths are between $1.973(5)$ and $1.983(5)$ Å, similar to previously reported Pd–C_{NHC} values.^[19,20,22]

The formation of the dimetallic species **9** may reflect the different electron density at palladium when bound to C4-bound dicarbene as compared to C2-bound analogues (cf. formation of **4a** from the BF₄ salt **3c**). Apparently the palladium(II) center is less electron-deficient when coordinated by two C4-bound carbene and is therefore sufficiently stabilized by two μ^2 -bound chloride ligands, whereas with C2-bound dicarbene ligands the stronger donating μ^1 -bonding mode of the chlorides is preferred.

Structural impact of the carbene bonding mode: To identify the structural consequences of C2 versus C4 bonding of the dicarbene ligand, the molecular structures of **4a**, **4b**, **8a**, and **8b** were determined by single-crystal X-ray diffraction (Figure 3). Selected bond lengths and angles are listed in

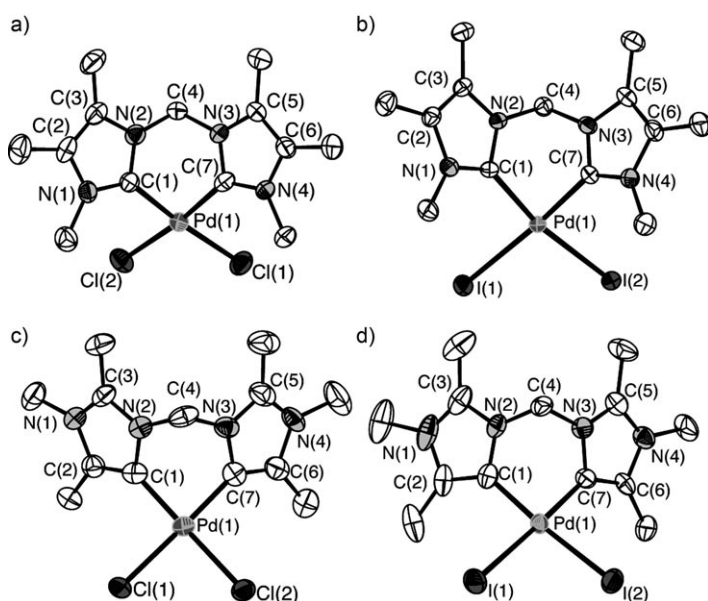


Figure 3. Molecular structure of complexes **4a** (a), **4b** (b), **8a** (c), and **8b** (d) (ORTEP representation, 50% probability level, hydrogen atoms and co-crystallized solvent molecules omitted for clarity).

Table 1. In all complexes the palladium center resides in a distorted square-planar configuration. The Pd–C bond length is slightly shorter in the chloride complexes **4a** and **8a** than in the iodide analogues **4b** and **8b**, perhaps due to the higher *trans* influence of iodide versus chloride. In contrast the carbene bonding mode seems to have no influence on the Pd–C bond length, all Pd–C distances are around the expected value of 1.98(2) Å.^[19,20,22] Notably, the Pd–Cl bonds are significantly longer in the abnormal complex **8a** than in **4a**, suggesting a higher *trans* influence of C4-bound carbenes. No such trend is observed for the palladium–

Table 1. Selected bond lengths [Å] and angles [°] in complexes **4a**, **8a**, **4b**, and **8b**.

	4a X = Cl	8a X = Cl	4b X = I	8b X = I
Pd(1)–C(1)	1.979(4)	1.976(9)	2.007(4)	2.007(7)
Pd(1)–C(7)	1.976(5)	1.981(9)	1.981(4)	1.993(8)
Pd(1)–X(1)	2.3587(12)	2.400(2)	2.6648(5)	2.6734(9)
Pd(1)–X(2)	2.3556(13)	2.407(2)	2.6717(4)	2.6646(8)
C _{imi} –C _{imi} ^[a]	1.342(7)	1.353(13)	1.361(6)	1.363(12)
C _{imi} –C _{imi} ^[b]	1.349(6)	1.355(13)	1.355(6)	1.390(11)
C(1)–Pd(1)–C(7)	92.02(12)	86.1(4)	82.62(16)	84.6(3)
X(1)–Pd(1)–X(2)	90.89(5)	88.55(8)	93.693(14)	89.80(3)
N(2)–C(1)–Pd(1)–C(7)	42.7(4)	–43.5(7)	47.6(3)	–40.7(6)
C(1)–Pd(1)–C(7)–N(3)	–44.8(4)	38.9(7)	–48.3(3)	45.0(6)

[a] C_{imi}–C_{imi} is C(2)–C(3) for **4** and C(1)–C(2) for **8**. [b] C_{imi}–C_{imi} is C(5)–C(6) for **4** and C(6)–C(7) for **8**.

iodide bonds in **4b** and **8b**, probably due to steric repulsion between the large iodide nucleus and the CH₃ group in *ortho* position (attached to N3 and C5 respectively). The heterocyclic C–C bond tends to be slightly longer in abnormally bound carbenes (av 1.365(17) Å) than in normal C2-bound carbene complexes (av 1.352(8) Å), though the effect is much less pronounced than in C5-protonated analogues.^[22] The torsion between the palladium square plane and the heterocycles as defined by the N–C–Pd–C dihedral angles varies in the 38–48° range and is essentially independent of the carbene bonding mode.

The conformational similarity of the two dicarbene ligands in complexes **4a** and **8a** is further illustrated by the superimposition of the two molecular structures (Figure 4).

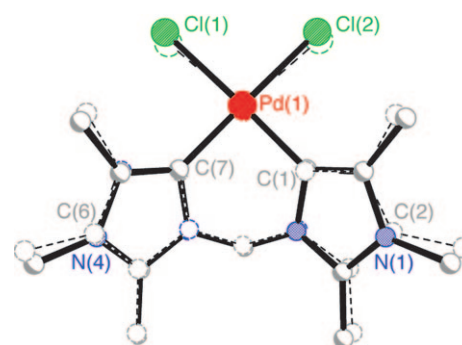


Figure 4. Superimposition of the molecular structures of **4a** (dashed) and **8a** (solid) using the C(1)–Pd(1)–C(7) plane as a reference.

Using the C(1)–Pd(1)–C(7) bonding as anchoring point, only slight deviations in the ligand periphery are detectable, arising predominantly from the relative orientation of the heterocycles with respect to the metal coordination plane. Minor differences are also noted in the N–CH₃ versus C–CH₃ bond lengths. For example the N(1)–CH₃ distance in **4a** is 1.403(6) Å, whereas the C(2)–CH₃ bond length is 1.481(14) Å in **8a**. Since these structural differences are very small only, it is probably safe to ignore any stereoelectronic contributions and to attribute the diverting reactivity and stability patterns of the complexes to the *electronic* impact of the carbene bonding mode.

X-ray photoelectron spectroscopy: The variation of electron density at the palladium center as a consequence of the different carbene bonding in complexes **4a** and **8a** was probed by X-ray photoelectron spectroscopy (XPS). Quantitative analyses of the measurements were complicated by the fact that both complexes were charged under XPS conditions, which required appropriate referencing. When taking the average kinetic energy of the 1s electrons of C, N, and O as a reference, the binding energy of the palladium 3d electrons in **8a** is 0.5 eV lower than that of palladium in a C2-bound dicarbene environment as in **4a** (Figure 5). This implies a higher electron density at the palladium when bound to abnormal C4-bound carbenes and corroborates previous analysis using structurally less similar C2- and C4-bound di-

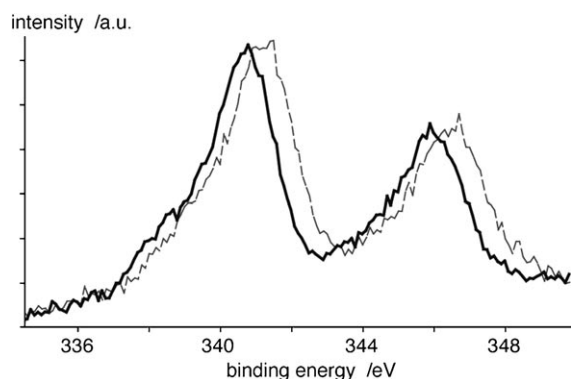
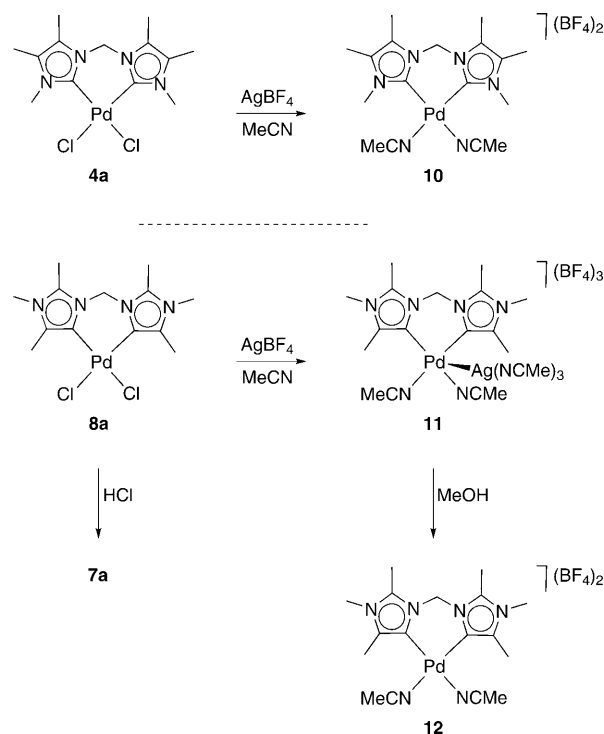


Figure 5. XPS spectra (palladium 3d level) for the C2-bound dicarbene complex **4a** (dashed) and the C4-bound analogue **8a** (solid line).

carbene palladium (II) complexes.^[3b] Independent DFT calculation of the binding energy of the palladium 3d electrons revealed a 0.8 eV lower energy in abnormally bound dicarbene complexes than in the normal analogue (336.1 eV vs. 336.9 eV). The slight shift in absolute energies may be attributed to the charging of the complexes under experimental conditions. These XPS measurements are in line with earlier IR analyses of ν_{CO} stretching frequencies in abnormal carbene iridium dicarbonyl complexes,^[3a] and they demonstrate unequivocally that C4-bound carbenes are exceptionally strong donors^[24] and considerably stronger than their C2-bound analogues.

Impact of carbene C4-bonding on reactivity: The steric similarity of complexes **4** and **8** also allowed the investigation of the relevance of electronic effects on the reactivity of the coordinated metal centers. Upon reaction of complex **8** with AgBF_4 , the silver adduct **11** was isolated, whereas the normally bound dicarbene complex **4** only underwent halide abstraction and gave the bis-solvento complex **10** (Scheme 2; Figure 6a). Formation of such a bimetallic complex **11** suggests that $\text{Pd}\cdots\text{Ag}$ bond formation is a general process in C4-bound carbene palladium complexes.^[3b] This behavior may become attractive for exploiting new types of direct metal–metal interactions.^[25]

A crystal structure analysis of the bimetallic complex **11** revealed that, most notably, the $\text{Pd}\cdots\text{Ag}$ bond length is significantly longer (3.1120(10) Å; Figure 6b) than in a related complex comprising a proton at the C5 position ($\text{Pd}\cdots\text{Ag}$ 2.8701(6) Å).^[3b] Presumably, this is a consequence of the different steric repulsion between the C5-bound substituent (crystallographically labeled C(2) and C(6) in Figure 6b) and the acetonitrile ligands around the silver nucleus. The silver ion is significantly shifted towards the carbene ligands, which is reflected by the acute $\text{Ag-Pd-C}_{\text{carbene}}$ angles ($\text{Ag}(1)\text{-Pd}(1)\text{-C}(1)$ 64.6(2)° and $\text{Ag}(1)\text{-Pd}(1)\text{-C}(7)$ 64.7(2)°). This bonding situation compares well with that in the previously reported $\text{Ag-Pd}(\text{dicarbene})$ complex with a proton at the C5-position,^[3b] which shows $\text{Ag-Pd-C}_{\text{carbene}}$ angles of 65.8(2) and 68.3(1)°.



Scheme 2. Reactivity patterns of normal and abnormal dicarbene complexes towards Lewis and Brønsted acids.

The observed geometry indicates that silver bonding occurs not only via the d_{z^2} orbital of the palladium center, expected to be the HOMO within the $\text{Pd}(\text{dicarbene})$ fragment, since such a donor interaction should position the silver nucleus in an apical position. Significant donor contributions may also originate from the palladium–carbene bonds, either by an agostic bonding (i.e., electron density from the Pd-C σ bond) or by interaction with the Pd=C π bond. Theoretical analyses using BP86/TZ2P suggested that the two metal fragments of complex **11** dissociate spontaneously in the gas phase. No minimum could be located on the potential energy surface that would be close to the crystallographically characterized structure. Optimization of the structure with constrained Ag-Pd and $\text{Ag}\cdots\text{C}$ distances based on the crystallographically determined values allowed, however, the identification of the relevant bonding interactions. Accordingly, substantial stabilization of the silver cation arises from orbital interactions between the filled d_{z^2} orbital of palladium and the LUMO of Ag^+ (predominantly s character, $\Delta E = -12 \text{ kcal mol}^{-1}$). A weaker interaction of $-4.4 \text{ kcal mol}^{-1}$ involves electron donation from a silver 4d orbital to the Pd-C π^* orbital (Figure 7). While this contribution is relatively small, it may rationalize the observed shift of the silver ion from the palladium z axis towards the dicarbene ligand. Furthermore, these calculations reveal 1 eV higher energy levels for the carbene orbitals in the C4 coordination mode as compared to that in 2-imidazolylienes. This energy difference indicates a substantially larger charge transfer from the carbene lone pair to the coordinated metal center when bound via C4 and may hence provide

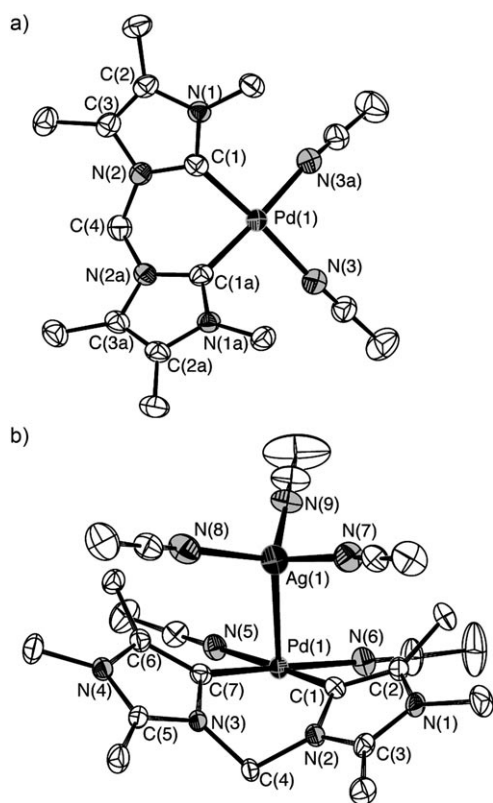


Figure 6. Reaction products from the reaction of C2- and C4-bound dicarbene palladium complexes with AgBF_4 in MeCN. Molecular structure of the cationic portions of complexes **10** (a) and **11** (b; ORTEP representation, 50 % probability, hydrogen atoms, non-coordinating BF_4^- anions and cocrystallized solvent molecules omitted for clarity). Selected bond lengths [Å] and angles [°]: for **10**: Pd1–C1 1.955(4), Pd1–N3 2.071(4); C1–Pd1–C1a 83.2(2), C1–Pd1–N3 173.40(15), C1–Pd1–N3a 4.70(15), N3–Pd1–N3a 86.72(19). For **11**: Pd1–Ag1 3.1120(10), Pd1–C1 1.970(7), Pd1–C7 1.966(7), Pd1–N5 2.075(6), Pd1–N6 2.082(7), C1–C2 1.367(9), C6–C7 1.373(10); C1–Pd1–C7 85.8(3), Ag1–Pd1–C1 64.6 (2), Ag1–Pd1–C7 64.68(18).

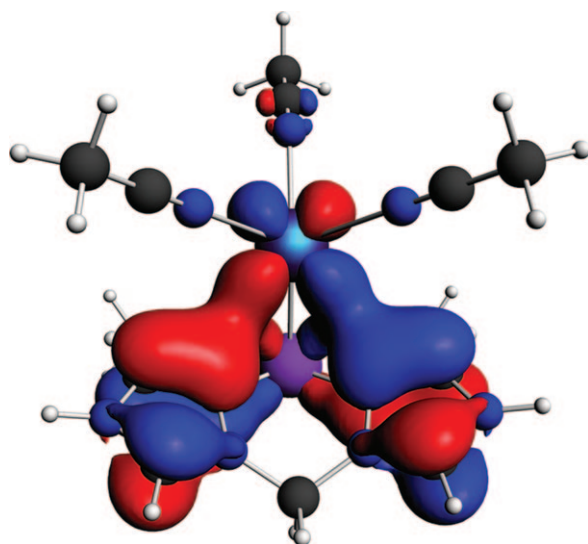
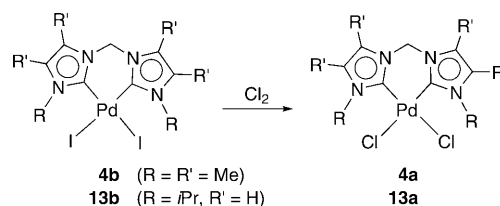


Figure 7. Calculated interactions that are relevant for stabilizing the silver cation in the bimetallic complex **11** (color code: Pd purple, Ag light blue, N blue, C gray).

a rational explanation for the enhanced nucleophilicity of the palladium center in complexes **8**.

Similarly to the reaction with Lewis acidic Ag^+ , complexes **8** comprising C4-bound dicarbenes also react with strong Brønsted acids. Both Pd–C bonds in **8** are acid sensitive and are cleaved within minutes. For example, exposure of complex **8a** to HCl (0.4 M in MeCN) led to the rapid acidolysis and formation of the imidazolium salt **7a**. A similar reaction outcome was observed when using H_2SO_4 , while complexes **4a** and **4b** are stable for weeks under such acidic conditions, even upon heating to 80 °C. Clearly, steric protection of the palladium center and of the Pd–C bonds can be excluded as an argument for rationalizing this distinctly different reactivity of C2- and C4-bound dicarbene complexes. Possibly, oxidative addition of HX and subsequent reductive elimination of an imidazolium cation from a putative $\text{Pd}^{\text{IV}}(\text{dicarbene})(\text{hydride})$ intermediate may occur. Reductive carbene elimination is known to be promoted by C4-bound carbene ligands.^[26] Alternatively, a Lewis acid/base adduct similar to the silver complex **11** may form, in which the proton is located at a similar position as Ag^+ in **11** and hence in close proximity to both Pd–C bonds. Subsequent rearrangement of such an intermediate into a Pd···H···C three-center, two-electron transition state followed by thermodynamically driven metal–carbon bond breaking is then conceivable. Irrespective of the exact mechanism, the acid lability and the nucleophilic character of the palladium center in **8** appeared to be a direct consequence of the ligand-induced difference of electron density, both at the metal center and at the metal-bound carbon.

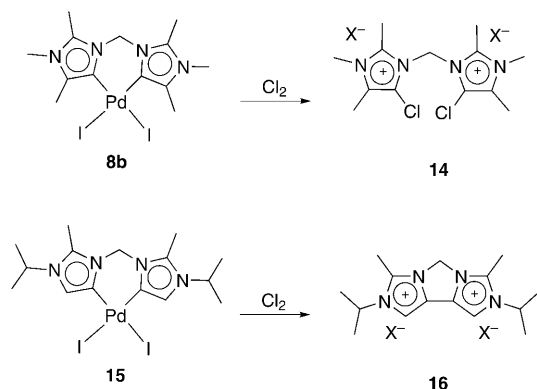
Based on the exceptionally high donor ability of C4-bound carbenes, the palladium centers in **8** are expected to promote redox reactions considerably better than in **4**, comprising normally bound carbene ligands. We have probed such reactivity patterns by exposing different palladium complexes to a Cl_2 atmosphere. Under these conditions, the C2-bound dicarbene systems **4b** and **13b** underwent halide metathesis and afforded complexes **4a** and **13a**, respectively, containing metal-bound chlorides (Scheme 3). Substitution of the metal-bound halides was confirmed by a diagnostic shift of the metal-bound carbon in the ^{13}C NMR spectrum, for example, in complex **13** from $\delta_{\text{C}} = 162.5$ to 156.5 ppm. Similarly the isopropyl protons are displaced in the ^1H NMR spectrum from $\delta_{\text{H}} = 5.37$ to 5.53 ppm, probably due to intramolecular hydrogen bonding of the isopropyl protons to the metal-bound halides.^[19b] The structure of **13a** was further confirmed by crystallographic analysis.^[23] Mech-



Scheme 3. Reactivity of normal dicarbene complexes towards molecular chlorine.

anistically, formation of the chloride complex may be rationalized by an oxidative addition of Cl_2 to the palladium center followed by reductive I_2 or ICl elimination. In the presence of excess Cl_2 , the postulated palladium(IV) oxidative addition product $[\text{PdCl}_4(\text{dicarbene})]$ is apparently unstable and reverts back to complex **13a**.

In contrast, the C4-bound carbene complex **8b** afforded the dichloro diimidazolium salt **14** upon exposure to Cl_2 (Scheme 4). While the removal of I_2 may proceed according



Scheme 4. Reactivity of abnormal dicarbene complexes towards molecular chlorine ($\text{X}^- = [\text{PdCl}_3(\text{DMSO})]^-$ or $0.5[\text{PdCl}_4]^{2-}$).

to a process similar to that suggested for **4b**, apparently reductive elimination of $\text{C}_{\text{NHC}}-\text{Cl}$ is relatively facile in C4-bound carbene palladium(IV) complexes. In solution, probably $[\text{PdCl}_4]^{2-}$ is formed initially as anion of the dichloro diimidazolium salt and perturbation of the original 2:1 imidazolium/palladium stoichiometry occurred only upon recrystallization from DMSO solution. Both elemental analyses and a crystal structure determination (Figure 8a) of recrystallized samples indicated a 4:3 imidazolium/palladium ratio due to the presence of one $[\text{PdCl}_4]^{2-}$ and two $[\text{PdCl}_3(\text{DMSO})]^-$ ions, and two diimidazolium dications. Reductive elimination of the carbene ligand was also observed from the C5-protonated dicarbene palladium complex **15** in the presence of excess Cl_2 (Scheme 4). Demetallation occurred, however, not via $\text{C}_{\text{NHC}}-\text{Cl}$ bond formation but via $\text{C}_{\text{NHC}}-\text{C}_{\text{NHC}}$ bond making, thus affording the tricyclic diimidazolium salt **16** (Figure 8b). The molecular structure of this diimidazolium salt revealed a strained arrangement of the heterocycles as reflected by the $\text{C}(3)-\text{C}(4)-\text{C}(5)$ bond angle of $147.3(9)^\circ$, which is unusually large for a formally sp^2 -hybridized carbon center. The ^{13}C NMR resonance of the bridging C4 nucleus was observed in the usual region ($\delta_{\text{C}} = 123.5$ ppm), while the remarkable high-field shift of the resonance due to the proton-bound C5 carbon ($\delta_{\text{C}} = 111.9$ ppm) may reflect the strained geometry. In the ^1H NMR spectrum of **16**, the signal attributed to the aromatic proton is displaced to lower field ($\delta_{\text{H}} = 7.16$ ppm in **15** versus $\delta_{\text{H}} = 8.34$ ppm in **16**). The presence of only little steric bulk at C5 in complex **15** as compared to the permethylated ligand in complex **8** may play a key role for distinguishing the out-

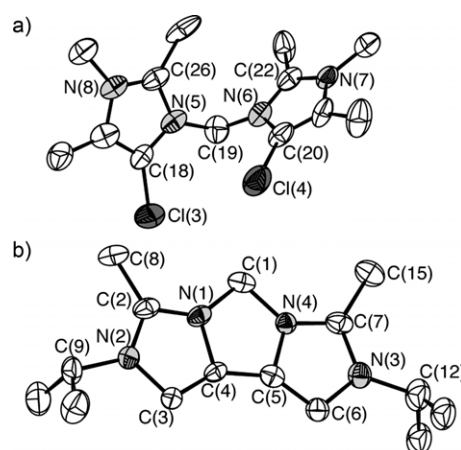


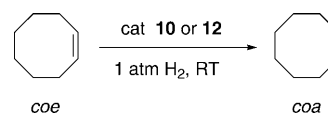
Figure 8. Molecular structure of a) one of the crystallographically independent dications of **14**, and b) one of the two cationic portions of compound **16**, (ORTEP representation, 50% probability, $[\text{PdCl}_4]^{2-}$ and $[\text{PdCl}_3(\text{DMSO})]^-$ ions omitted for clarity). Selected bond lengths [\AA] for **14**: $\text{C}(18)-\text{C}(27)$ 1.341(14), $\text{C}(20)-\text{C}(21)$ 1.340(14), $\text{C}(18)-\text{C}(13)$ 1.692(10), $\text{C}(20)-\text{C}(14)$ 1.668(10). Selected bond lengths [\AA] and angles [$^\circ$] for **16**: $\text{C}(3)-\text{C}(4)$ 1.336(13), $\text{C}(4)-\text{C}(5)$ 1.433(14), $\text{C}(5)-\text{C}(6)$ 1.345(15); $\text{N}(4)-\text{C}(1)-\text{N}(1)$ 99.3(7), $\text{C}(3)-\text{C}(4)-\text{N}(1)$ 107.4(8), $\text{C}(3)-\text{C}(4)-\text{C}(5)$ 147.3(9), $\text{C}(5)-\text{C}(4)-\text{N}(1)$ 105.3(8), $\text{C}(6)-\text{C}(5)-\text{N}(4)$ 108.3(8), $\text{C}(6)-\text{C}(5)-\text{C}(4)$ 145.4(9), $\text{C}(4)-\text{C}(5)-\text{N}(4)$ 106.3(8).

come of the reductive elimination processes. The methyl groups at C5 in complex **8a** and in the putative Pd^{IV} intermediate may be sterically too demanding to allow an arrangement of the two carbene ligands that would induce $\text{C}-\text{C}$ reductive elimination as observed from complex **15**.

Reductive carbene elimination and formation of **14** and **16** is in agreement with previous findings, which indicated that C4-bound carbene ligands are more prone to reductively eliminate from M^{II} centers than the C2-bound analogues ($\text{M} = \text{Ni}, \text{Pd}, \text{Pt}$).^[26] Based on our observations, reductive elimination from Pd^{IV} decreases in the sequence $\text{I}-\text{I} > \text{C}_{\text{carb}}-\text{C}_{\text{carb}} > \text{C}_{\text{carb}}-\text{Cl} \gg \text{C}_{\text{carb}}-\text{C}_{\text{carb}}$. Clearly, further mechanistic and theoretical investigations are warranted to substantiate this trend.

Catalysis: The electronic implications due to the different carbene bonding have also significant consequences on the catalytic activity of the coordinated metal center. This impact has been observed with sterically less similar dicarbene complexes. Here, it is illustrated by the distinctly different performance of complexes **10** and **12** as catalyst precursors for alkene hydrogenation (Scheme 5).

Hydrogenation of cyclooctene (coe) to cyclooctane (coa) was used as a model reaction. Catalytic runs were performed at room temperature and under atmospheric pres-



Scheme 5. Palladium(dicarbene)-catalyzed olefin hydrogenation.

sure of H₂. Under these conditions, the C4-bound carbene complex **12** showed appreciable catalytic activity, conversions reached 57% after 1 h and were essentially complete after 8 h. In contrast, the C2-bound analogue **10** is inactive and even after 20 h, no coa was formed. These results are in line with our preliminary studies on the hydrogenation of coe,^[3b] which suggested that the C4-carbene bonding mode is pivotal for imposing high catalytic activity. Steric modifications appear to play only a minor role yet they may become relevant for catalyst optimization. Assuming that catalytic hydrogenation involves oxidative addition of H₂ to the metal center,^[27] the high catalytic activity of **12** may be rationalized by the substantial electron density at the palladium center as a consequence of the exceptionally strong donor ability of the two C4-bound carbene ligand residues. Furthermore, reductive elimination of either the product or the heterocycle may occur,^[28] in analogy to the specific reactivity patterns established for the reaction of C4-bound carbene complexes with Cl₂ (see above). The latter reaction trajectory may generate a palladium polyhydride species as the catalytically active species. Mechanistic studies directed towards a better understanding of this palladium-catalyzed hydrogenation are currently ongoing in our laboratories.

Conclusion

Palladium complexes comprising sterically strongly related dicarbene ligands that bind the metal center either normally at C2 or abnormally at C4 allowed unambiguous identification of the electronic impact of the abnormal bonding mode of imidazolyldienes. In the solid state, carbene bonding at the C4 position induces a higher *trans* influence and an increased electron density at the metal center. In solution the stability towards Lewis and Brønsted acids is reduced, and the reactivity towards Cl₂ and in catalytic olefin hydrogenation is considerably higher. All evidence suggests that C4-bound dicarbene complexes are markedly stronger donors than their C2-bound analogues. Enhanced donation of C4-bound imidazolyldienes may be rationalized, in analogy to C2-bound carbene systems, by a partition of the heterocyclic π -electron density into an NCN amidinium fragment and a C=C portion. The latter includes in C4-bound imidazolyldienes also the coordinated metal center. Such a notion features a ground state comprising a vinyl-type anionic site, which is stabilized by an intramolecularly confined amidinium cation.

Furthermore, the differences of the reactivity patterns of C2- and C4-bound imidazolyldienes appear to be predominantly electronic in origin. Consequently, steric protection of the metal center and likewise of the metal–carbene bond by *ortho* substituents (namely, at N3 for C2-bound imidazolyldienes, and at C5 for C4-bound imidazolyldienes) does not alternate the reactivity patterns substantially, though the activity may be influenced. Most importantly, abnormal dicarbene bonding renders a typically electrophilic metal center such as palladium(II) into a nucleophilic site. Efforts in our laboratories are currently directed towards exploiting

the strong donor ability of C4-bound carbenes, in particular for the activation of less reactive C–H bonds.

Experimental Section

General: The syntheses of the dimethyl imidazole **1**^[16] and of the palladium complexes **13b**^[19b] and **15**^[3b] were reported previously. All other reagents are commercially available and were used as received. All NMR spectra were recorded on Bruker spectrometers at 25°C unless specified otherwise. The ¹H and ¹³C chemical shifts (δ in ppm, coupling constants *J* in Hz) were referenced to external SiMe₄. Assignments are based on homo- and heteronuclear shift correlation spectroscopy. Elemental analyses were performed by the Microanalytical Laboratory of Ilse Beetz (Kronach, Germany) or the Microanalytical Laboratory of the ETH (Zürich, Switzerland). Microwave-mediated reactions were carried out on a Biotage Initiator 2.0 instrument. The XPS spectra were measured on a Scienta SES 2002 electron spectrometer with a 5×10^{-11} mbar base pressure. The photon source consisted of an X-ray tube emitting MgK α photons at 1253.6 eV.

Synthesis of 2: CH₃I (4.31 g, 30.4 mmol) was added to a solution of 4,5-dimethylimidazole **1** (2.60 g, 27.4 mmol) in DMSO (100 mL). Powdered KOH (3.42 g, 61.0 mmol) was then added in small quantities and the solution was stirred at room temperature for 1 h and at 65°C for 18 h. After the mixture had been cooled to room temperature, KOH (100 mL, 1 M) was added and the product was extracted with CH₂Cl₂ (3 \times 100 mL). The combined organic phases were washed with KOH (100 mL), H₂O (2 \times 100 mL), and brine (2 \times 100 mL), dried over Na₂SO₄, and evaporated under reduced pressure to give trimethylimidazole **2** (1.31 g, 44%). ¹H NMR (360 MHz, CDCl₃): δ = 7.21 (s, 1H, H_{imi}), 3.41 (s, 3H, NCH₃), 2.07, 2.03 ppm (2 \times s, 6H, C_{imi}–CH₃); ¹³C{¹H} NMR (90 MHz, CDCl₃): δ = 135.1 (C_{imi}–H), 133.5, 122.5 (2 \times C_{imi}), 31.3 (NCH₃), 12.7, 8.1 ppm (2 \times C_{imi}–CH₃).

Synthesis of 3a: A solution of **2** (2.20 g, 20.0 mmol) and CH₂Cl₂ (3 mL) was stirred at 150°C under microwave irradiation for 30 min. A brown oil had formed, which was separated by decantation and washed with toluene (3 \times 20 mL) and Et₂O (3 \times 20 mL) and then dried in vacuo to give **3a** as brown solid (2.39 g, 78%) as a highly viscous oil. All our attempts to crystallize **3a** at –30°C under various conditions have failed thus far and elemental analysis was only satisfactory when including solvents. ¹H NMR (500 MHz, [D₆]DMSO): δ = 9.53 (s, 2H, H_{imi}), 6.75 (s, 2H, NCH₂N), 3.78 (s, 6H, NCH₃), 2.31, 2.22 ppm (2 \times s, 12H, C_{imi}–CH₃); ¹³C{¹H} NMR (125 MHz, [D₆]DMSO): δ = 136.5 (C_{imi}–H), 128.3, 126.3 (2 \times C_{imi}), 55.1 (CH₂), 33.9 (NCH₃), 8.2, 7.7 ppm (2 \times C_{imi}–CH₃); elemental analysis calcd (%) for C₁₃H₂₂Cl₂N₄ (305.25): 2 H₂O \cdot 0.5 CH₂Cl₂: C 42.25, H 7.09, N 14.60; found: C 42.88, H 7.46, N 14.74.

Synthesis of 3b: A solution of **2** (1.60 g, 5.97 mmol) and CH₂I₂ (1.31 g, 11.9 mmol) in toluene (20 mL) was stirred at reflux for 14 h. A brown oil formed, which was separated by decantation and washed with toluene (3 \times 20 mL) and Et₂O (3 \times 20 mL), and then dried in vacuo to give **3b** as brown solid (1.54 g, 50%). ¹H NMR (500 MHz, [D₆]DMSO): δ = 9.27 (s, 2H, H_{imi}), 6.61 (s, 2H, NCH₂N), 3.78 (s, 6H, NCH₃), 2.30, 2.24 ppm (2 \times s, 12H, C_{imi}–CH₃); ¹³C{¹H} NMR (125 MHz, [D₆]DMSO): δ = 136.0 (C_{imi}–H), 128.3, 126.3 (2 \times C_{imi}), 55.3 (CH₂), 34.0 (NCH₃), 8.3, 7.9 ppm (2 \times C_{imi}–CH₃); elemental analysis calcd (%) for C₁₃H₂₂I₂N₄ (488.15): C 31.99, H 4.54, N 11.48; found: C 31.95, H 4.65, N 12.09.

Synthesis of 3c: A suspension of **3b** (1.09 g, 2.23 mmol) and AgBF₄ (0.92 g, 4.73 mmol) in MeCN (20 mL) was stirred at room temperature for 18 h in the absence of light. The suspension was then filtered through Celite and the volatiles were removed in vacuo to give **3c** as a red oil (0.87 g, 96%), which was recrystallized from MeOH/Et₂O. ¹H NMR (360 MHz, [D₆]DMSO): δ = 9.18 (s, 2H, H_{imi}), 6.56 (s, 2H, NCH₂N), 3.76 (s, 6H, NCH₃), 2.28 (s, 6H, C_{imi}–CH₃), 2.22 ppm (s, 6H, C_{imi}–CH₃); ¹³C{¹H} NMR (100 MHz, [D₆]DMSO): δ = 136.3 (C_{imi}–H), 128.4, 126.4 (2 \times C_{imi}), 55.1 (CH₂), 33.8 (NCH₃), 8.0, 7.6 ppm (2 \times C_{imi}–CH₃); elemental analysis calcd (%) for C₁₃H₂₂B₂F₈N₄ (407.95): C 38.27, H 5.44, N 13.73; found: C 38.45, H 5.31, N 13.43.

Synthesis 4a: Pd(OAc)₂ (0.19 g, 0.83 mmol) and excess of KCl (0.31 g, 4.15 mmol) was added to a solution of **3c** (0.34 g, 0.83 mmol) in DMSO (6 mL). The reaction mixture was heated at 50°C for 2 h and then at 120°C for 3 h. After the mixture had been cooled to room temperature, CH₂Cl₂ (20 mL) and Et₂O (80 mL) were added. A precipitate appeared which was collected and washed repeatedly by adding CH₂Cl₂ (20 mL) followed by precipitation with Et₂O (80 mL). After drying in vacuo, **4a** was obtained as an off-white powder (0.28 g, 83%). An analytically pure sample was obtained by recrystallization of **4a** from CH₃NO₂/Et₂O. ¹H NMR (500 MHz, [D₆]DMSO): δ = 6.04, 5.85 (2 × AB, ²J_{HH} = 13.8 Hz, 2H, CH₂), 3.78 (s, 6H, NCH₃), 2.23, 2.09 ppm (2 × s, 12H, C_{imi}-CH₃); ¹³C{¹H} NMR (125 MHz, [D₆]DMSO): δ = 155.8 (C-Pd), 125.9, 124.3 (2 × C_{imi}), 57.1 (CH₂), 40.4 (NCH₃), 8.4, 8.2 ppm (2 × C_{imi}-CH₃); elemental analysis calcd (%) for C₁₃H₂₀Cl₂N₄Pd (409.65): C 38.12, H 4.92, N 13.68; found: C: 38.08, H 4.93, N 13.54.

Synthesis of 4b: The method was analogous to the one described for the synthesis of **4a** except for the KCl, which was omitted. Starting from Pd(OAc)₂ (0.45 g, 2.0 mmol) and **3b** (1.0 g, 2.1 mmol), **4b** was obtained as an off-white solid (0.64 g, 55%). An analytically pure sample was obtained by recrystallization of **4b** from DMSO/Et₂O. ¹H NMR (500 MHz, [D₆]DMSO): δ = 6.06, 5.91 (2 × AB, ²J_{HH} = 14.2 Hz, 2H, CH₂), 3.69 (s, 6H, NCH₃), 2.24, 2.09 ppm (2 × s, 12H, C_{imi}-CH₃); ¹³C{¹H} NMR (125 MHz, [D₆]DMSO): δ = 161.1 (C-Pd), 126.0, 124.7 (2 × C_{imi}), 57.3 (CH₂), 40.4 (NCH₃), 8.5, 8.2 ppm (2 × C_{imi}-CH₃); elemental analysis calcd (%) for C₁₃H₂₀I₂N₄Pd (592.55)-0.25 Et₂O: C 28.51, H 4.20, N 8.99; found: C: 28.20, H 3.93, N 8.81.

Synthesis of 6: A mixture of acetic anhydride (2.5 g, 25 mmol) and 2,4-dimethylimidazole **5** (0.93 g, 10 mmol) in benzene (10 mL) was stirred at 80°C for 2 h. Then MeI (0.6 mL, 9.6 mmol) in benzene (6 mL) was added and the mixture was stirred at 140°C in a sealed tube. After 16 h, the reaction was quenched with water and aqueous KOH (1 M, 100 mL) was added until pH > 10. The product was extracted with CH₂Cl₂ (3 × 100 mL). The combined organic phases were washed with aqueous KOH (1 M, 100 mL), H₂O (2 × 100 mL) and brine (2 × 100 mL), dried over Na₂SO₄, and evaporated to dryness, thus affording **6** as a colorless oil (0.70 g, 64%). An analytically pure sample was obtained from the corresponding HCl salt upon recrystallization from MeOH/Et₂O. ¹H NMR (500 MHz, CDCl₃): δ = 6.60 (s, 1H, H_{imi}), 3.38 (s, 3H, NCH₃), 2.34, 2.14 ppm (2 × s, 6H, C_{imi}-CH₃); ¹³C{¹H} NMR (125 MHz, CDCl₃): δ 144.3, 127.4 (2 × C_{imi}), 116.7 (C_{imi}-H), 29.8 (NCH₃), 13.63, 9.92 ppm (2 × C_{imi}-CH₃); elemental analysis calcd (%) for C₆H₁₁ClN₂ (146.62)-0.5 H₂O: C 46.31, H 7.77, N 18.00; found: C: 46.26, H 7.13, N 17.29.

Synthesis of 7a: A solution of **6** (1.1 g, 10.0 mmol) in CH₂Cl₂ (5 mL) was stirred in a sealed tube at 150°C under microwave irradiation for 30 min. A red oil formed, which was separated by precipitation with MeOH (20 mL) and Et₂O (80 mL). The residue was washed once more with MeOH (20 mL) and Et₂O (80 mL) to give **7a** (1.15 g, 75%) as a highly viscous oil. Attempts to crystallize **7a** under various conditions for microanalysis have failed thus far. ¹H NMR (500 MHz, [D₆]DMSO): δ = 7.85 (s, 2H, H_{imi}), 6.90 (s, 2H, CH₂), 3.66 (s, 6H, NCH₃), 2.83, 2.25 ppm (2 × s, 12H, C_{imi}-CH₃); ¹³C{¹H} NMR (125 MHz, [D₆]DMSO): δ = 145.6, 130.7 (2 × C_{imi}), 130.7 (2 × C_{imi}), 117.6 (C_{imi}-H), 56.4 (CH₂), 32.2 (NCH₃), 10.9, 9.2 ppm (2 × C_{imi}-CH₃).

Synthesis of 7b: Neat CH₂I₂ (1.9 g, 7.2 mmol) was added to **6** (1.40 g, 12.7 mmol) and the mixture was stirred at 140°C for 16 h. The formed brown oil was dissolved in MeOH (20 mL). Upon addition of Et₂O (80 mL), crude **7b** separated as an reddish oil, which was collected by decantation and dried in vacuo (2.2 g, 63%). Recrystallization from MeOH/Et₂O gave **7b** as an analytically pure solid. ¹H NMR (500 MHz, [D₆]DMSO): δ = 7.61 (s, 2H, H_{imi}), 6.57 (s, 2H, CH₂), 3.66 (s, 6H, NCH₃), 2.76, 2.26 ppm (2 × s, 12H, C_{imi}-CH₃); ¹³C{¹H} NMR (125 MHz, [D₆]DMSO): δ = 145.6, 130.7 (2 × C_{imi}), 117.4 (C_{imi}-H), 56.3 (CH₂), 32.2 (NCH₃), 10.8, 9.1 ppm (2 × C_{imi}-CH₃); elemental analysis calcd (%) for C₁₃H₂₂I₂N₄ (488.15): C 31.99, H 4.54, N 11.48; found: C: 32.00, H 4.60, N 11.48.

Synthesis of 7c: A suspension of **7a** (2.21 g, 4.53 mmol) and AgBF₄ (1.86 g, 9.55 mmol) in MeCN (20 mL) was stirred at room temperature for 16 h in the absence of light. The suspension was then filtered through

Celite and the volatiles were removed in vacuo to give **7c** as a red oil (1.57 g, 85%). Microanalytically pure material formed upon crystallization of **7c** from MeOH/Et₂O. ¹H NMR (360 MHz, [D₆]DMSO): δ = 7.52 (s, 2H, H_{imi}), 6.50 (s, 2H, CH₂), 3.59 (s, 6H, NCH₃), 2.71 (s, 6H, C_{imi}-CH₃), 2.24 ppm (s, 6H, C_{imi}-CH₃); ¹³C{¹H} NMR (125 MHz, [D₆]DMSO): δ = 145.7, 130.9 (2 × C_{imi}), 117.4 (C_{imi}-H), 56.2 (CH₂), 31.9 (NCH₃), 10.2, 8.9 ppm (2 × C_{imi}-CH₃); elemental analysis calcd (%) for C₁₃H₂₂B₂F₈N₄ (407.95)-H₂O: C 36.66, H 5.68, N 13.15; found: C: 36.25, H 5.36, N 12.76.

Synthesis of 8a: Solid Pd(OAc)₂ (0.75 g, 3.36 mmol) was added to a solution of **7a** (0.56 g, 1.84 mmol) in DMSO (6 mL). The reaction mixture was stirred at 50°C for 2 h and then at 120°C for 3 h. After the mixture had been cooled to room temperature, CH₂Cl₂ (20 mL) and Et₂O (80 mL) were added to give a precipitate which was collected and washed repeatedly by adding CH₂Cl₂ (20 mL) followed by precipitation with Et₂O (80 mL) and dried in vacuo. This afforded **8a** as a yellow powder (0.49 g, 65%). An analytically pure sample of **8a** was obtained by recrystallization from CH₃NO₂/Et₂O. ¹H NMR (500 MHz, [D₆]DMSO): δ = 6.33, 5.93 (2 × AB, ²J_{HH} = 12.9 Hz, 2H, CH₂), 3.50 (s, 6H, NCH₃), 2.63 (s, 6H, C_{imi}-CH₃), 2.31 (s, 3H, C_{imi}-CH₃), 2.21 ppm (s, 6H, C_{imi}-CH₃); ¹³C{¹H} NMR (125 MHz, [D₆]DMSO): δ = 145.6, 130.7 (2 × C_{imi}), 117.4 (C-Pd), 56.3 (CH₂), 32.2 (NCH₃), 10.8, 9.1 ppm (2 × C_{imi}-CH₃); elemental analysis calcd (%) for C₁₃H₂₀Cl₂N₄Pd(409.65)-H₂O-CH₃NO₂: C 35.39, H 5.17, N 13.76; found: C: 35.14, H 4.91, N 13.51.

Synthesis of 8b: Excess NBu₄I (0.52 g, 1.41 mmol) was added to a solution of **12** (0.21 g, 0.35 mmol) in MeCN (20 mL) and the mixture was stirred at room temperature for 1 h. Addition of Et₂O (80 mL) induced the formation of a red precipitate, which was washed repeatedly by adding MeCN (20 mL) followed by precipitation with Et₂O (80 mL). After drying in vacuo, **8b** was obtained as a reddish solid (0.16 g, 77%). An analytically pure sample was obtained by recrystallization of **8b** from DMSO/Et₂O. ¹H NMR (500 MHz, [D₆]DMSO): δ = 6.32, 5.96 (2 × AB, ²J_{HH} = 13.5 Hz, 2H, CH₂), 3.46 (s, 6H, NCH₃), 2.60, 2.19 ppm (2 × s, 6H, C_{imi}-CH₃); ¹³C{¹H} NMR (125 MHz, [D₆]DMSO): δ = 145.3, 131.6 (2 × C_{imi}), 123.3 (C-Pd), 60.3 (CH₂), 32.1 (NCH₃), 15.6 (C₅^{imi}-CH₃), 11.6 (C₅^{imi}-CH₃), 10.5 ppm (C_{imi}-CH₃); the two signals at δ_C = 15.6 and 11.6 ppm coalesce to a singlet at 338 K (δ_C = 13.0 ppm); elemental analysis calcd (%) for C₁₃H₂₀I₂N₄Pd(592.55)-0.5 DMSO: C 26.62, H 3.67, N 8.87; found: C: 26.30, H 3.66, N 8.67.

Synthesis of 9: Pd(OAc)₂ (0.50 g, 2.23 mmol) was added to a solution of **7c** (0.91 g, 2.23 mmol) and KCl (0.83 g, 11.1 mmol) in DMSO (6 mL), and the reaction mixture was stirred at 50°C for 2 h and then at 120°C for 3 h. After the mixture had been cooled to room temperature, CH₂Cl₂ (20 mL) and Et₂O (80 mL) were added and the formed precipitate was collected. Repeated precipitation from CH₂Cl₂ (20 mL) and Et₂O (80 mL) and subsequent drying yielded **9** as an off-white powder (0.73 g, 89%). Analytically pure material was obtained by recrystallization from CH₃NO₂/Et₂O. ¹H NMR (500 MHz, [D₆]DMSO): δ = 6.33, 5.94 (2 × AB, ²J_{HH} = 13.2 Hz, 2H, CH₂), 3.50 (s, 6H, NCH₃), 2.63 (s, 6H, C_{imi}-CH₃), 2.31 (s, 3H, C_{imi}-CH₃), 2.21 ppm (s, 3H, C_{imi}-CH₃); ¹³C{¹H} NMR (100 MHz, [D₆]DMSO): δ = 141.8, 141.7, 131.2, 130.5, 129.5 (5 × C_{imi}), 126.8 (br, C_{imi}), 59.6 (CH₂), 31.5 (NCH₃), 11.2, 10.0 ppm (2 × C_{imi}-CH₃); elemental analysis calcd (%) for C₂₆H₄₈B₂Cl₂F₈N₈Pd₂(922.00)-0.25 Et₂O: C 34.48, H 4.55, N 11.91; found: C: 34.30, H 4.91, N 11.72.

Synthesis of 10: A suspension of **4b** (0.10 g, 0.17 mmol) and AgBF₄ (0.099 g, 0.51 mmol) in MeCN (20 mL) was stirred for 18 h in the absence of light. The suspension was filtered through Celite and the volatiles were evaporated, yielding **10** as an orange solid (0.10 g, 99%). Recrystallization of **10** from MeCN/Et₂O gave an analytically pure sample. ¹H NMR (500 MHz, [D₆]DMSO): δ = 6.24, 5.92 (2 × AB, ²J_{HH} = 14.0 Hz, 2H, CH₂), 3.70 (s, 6H, NCH₃), 2.26, 2.12 ppm (2 × s, 6H, C_{imi}-CH₃); ¹³C{¹H} NMR (100 MHz, [D₆]DMSO): δ = 144.5 (C-Pd), 127.0, 126.0 (2 × C_{imi}), 57.0 (CH₂), 34.5 (NCH₃), 8.3, 8.3 ppm (2 × C_{imi}-CH₃); elemental analysis calcd (%) for C₁₇H₂₆B₂F₈N₆Pd(594.46)-0.25 Et₂O: C 35.27, H 4.69, N 13.71; found: C: 35.07, H 4.69, N 13.43.

Synthesis of 11: A suspension of **8a** (0.15 g, 0.36 mmol) and AgBF₄ (0.24 g, 1.10 mmol) in MeCN (20 mL) was stirred for 18 h at room temperature in the dark. The suspension was filtered through Celite and the volatiles were removed to leave **11** as an orange oil (0.31 g, 94%), which

was recrystallized from MeCN/Et₂O. ¹H NMR (400 MHz, CD₃CN): δ = 6.76 (bs, 2H, CH₂), 3.45 (s, 6H, NCH₃), 2.50, 2.21 ppm (2×s, 6H, C_{imi}-CH₃); ¹³C{¹H} NMR (100 MHz, [D₆]DMSO): δ = 143.5 (C_{imi}), 138.3 (C-Pd), 122.6 (C_{imi}), 40.6 (CH₂), 32.0 (NCH₃), 10.7, 10.3 (2×C_{imi}-CH₃).

Synthesis of 12: Compound **11** (0.31 g, 0.36 mmol) was stirred in MeOH (20 mL) for 5 min at room temperature. The resulting suspension was filtered through Celite. Upon addition of Et₂O (80 mL) complex **12** sepa-

rated as a red oil that was collected, dried (0.13 g, 62 %). ¹H NMR (500 MHz, [D₆]DMSO): δ = 6.2 (bs, 2H, CH₂), 3.51 (s, 6H, NCH₃), 2.63, 2.21 ppm (2×s, 6H, C_{imi}-CH₃); ¹³C{¹H} NMR (100 MHz, [D₆]DMSO): δ = 142.6 (C_{imi}), 130.5 (C-Pd), 118.2 (C_{imi}), 59.4 (CH₂), 31.6 (NCH₃), 10.5, 10.2 ppm (2×C_{imi}-CH₃).

Synthesis of 13a: Gaseous Cl₂ was passed through a solution of complex **13b** (0.14 g, 0.24 mmol) in MeCN (20 mL) for 5 min. After addition of

Table 2. Crystallographic data for the reported complexes.

	4a	4b	8a	8b	9
color, shape	colorless block	light yellow block	light yellow block	yellow plate	colorless block
crystal size [mm]	0.45 × 0.40 × 0.25	0.45 × 0.40 × 0.35	0.15 × 0.15 × 0.10	0.05 × 0.13 × 0.15	0.45 × 0.40 × 0.35
formula	C ₁₃ H ₂₀ Cl ₂ N ₄ Pd·NO ₂ CH ₃	C ₁₃ H ₂₀ I ₂ N ₄ Pd·0.5 C ₃ H ₁₀ O	C ₁₃ H ₂₀ Cl ₂ N ₄ Pd·C ₂ H ₆ OS	C ₁₃ H ₂₀ I ₂ N ₄ Pd·C ₂ H ₆ OS	C ₂₆ H ₄₀ B ₂ Cl ₂ F ₈ N ₈ Pd ₂ ·3·C ₂ H ₆ OS
M _r	470.67	629.59	487.76	670.66	1156.36
T [K]	173(2)	173(2)	173(2)	173(2)	173(2)
crystal system	monoclinic	monoclinic	orthorhombic	monoclinic	triclinic
space group	P2 ₁ /n (no. 14)	C2/c (no. 15)	Pbcn (no. 60)	P2 ₁ /c (no. 14)	P $\bar{1}$ (no. 2)
unit cell					
a [Å]	14.2930(18)	25.710(2)	15.7970(15)	9.5887(8)	7.4897(10)
b [Å]	10.7619(10)	10.3113(8)	14.0280(16)	16.8738(14)	10.9460(14)
c [Å]	14.4646(18)	19.5043(18)	17.6586(15)	14.0823(12)	15.312(2)
α [°]	90	90	90	90	103.614(15)
β [°]	90.482(15)	130.291(5)	90	108.189(7)	90.211(16)
γ [°]	90	90	90	90	104.008(15)
V [Å ³]	2194.5(4)	3944.1(6)	3913.2(7)	2164.6(3)	1181.3(3)
Z	4	8	8	4	1
ρ _{calcd} [g cm ⁻³]	1.425	2.121	1.656	2.058	1.626
μ [mm ⁻¹] (MoKα)	1.104	4.078	1.339	3.816	1.080
no. total/unique reflections	13813/4336	28778/5351	31563/3497	10488/2916	8519/3921
R _{int}	0.0552	0.033	0.1714	0.046	0.0491
transmission range	0.690–0.748	0.265–0.376	0.655–0.697	0.934–1.042	0.712–0.747
no. parameters/restraints	187/0	212/0	208/0	236/0	262/11
R ^[a] /R _w ^[b]	0.0396/0.0929	0.0359/0.0890	0.0638/0.1263	0.0370/0.0845	0.0594/0.1554
GOF	0.820	1.072	0.928	0.94	0.958
min/max resid density [e Å ⁻³]	−0.944/0.630	−1.036/1.486	−1.464/1.254	−1.06/0.71	−1.113/1.571

	10	11	14	16
color, shape	colorless rod	colorless rod	orange block	colorless rod
crystal size [mm]	0.45 × 0.40 × 0.35	0.35 × 0.20 × 0.15	0.50 × 0.45 × 0.40	0.30 × 0.15 × 0.10
formula	C ₁₇ H ₂₆ B ₂ F ₈ N ₆ Pd·CH ₃ CN	C ₂₃ H ₃₅ AgB ₃ F ₁₂ N ₉ Pd	C ₃₀ H ₅₂ Cl ₁₄ N ₈ O ₂ Pd ₃ S ₂	C ₃₂ H ₅₄ Cl ₉ N ₈ OPd _{2.5} S·H ₂ O
M _r	635.51	912.3	1436.42	1201.96
T [K]	173(2)	173(2)	173(2)	173(2)
crystal system	orthorhombic	monoclinic	monoclinic	monoclinic
space group	Pnma (no. 62)	P2 ₁ /c (no. 14)	P2 ₁ /c (no. 14)	P2 ₁ /n (no. 14)
unit cell				
a [Å]	8.5260(7)	13.2455(12)	12.2432(9)	19.0030(12)
b [Å]	12.4423(10)	22.5844(17)	11.9193(10)	10.6288(6)
c [Å]	24.696(3)	13.3309(10)	36.348(2)	24.0690(18)
α [°]	90	90	90	90
β [°]	90	116.575(6)	95.393(8)	101.050(6)
γ [°]	90	90	90	90
V [Å ³]	2619.8(4)	3566.5(5)	5280.8(7)	4771.3(5)
Z	4	4	4	4
ρ _{calcd} [g cm ⁻³]	1.611	1.699	1.807	1.673
μ [mm ⁻¹] (MoKα)	0.788	1.146	1.836	1.522
no. total/unique reflections	19660/2720	24876/6285	35447/8828	33458/8322
R _{int}	0.0439	0.0770	0.0757	0.1077
transmission range	0.772–0.821	0.740–0.811	0.480–0.561	0.639–0.878
no. parameters/restraints	179/5	394/8	465/0	495/0
R ^[a] /R _w ^[b]	0.0469/0.1286	0.0601/0.1515	0.0740/0.1987	0.0783/0.2087
GOF	1.070	0.948	0.902	0.983
min/max resid density [e Å ⁻³]	−1.391/1.235	−1.523/1.377	−1.200/3.249	−3.574/3.821

[a] $R_1 = \sum ||F_o| - |F_c|| / \sum |F_o|$ for all $I > 2\sigma(I)$. [b] $wR_2 = [\sum w(F_o^2 - F_c^2)^2 / \sum w(F_o^4)]^{1/2}$.

Et₂O (80 mL), an orange precipitate appeared that was collected by decantation and dried in vacuo. The crude title product (92 mg, 92%) was recrystallized from MeOH/DMSO/Et₂O. ¹H NMR (360 MHz, [D₆]DMSO): δ = 7.61 (s, 2H, H_{im}), 7.51 (s, 2H, H_{im}), 6.30, 6.22 (2×AB, ²J_{HH} = 12.9 Hz, 2H, CH₂), 5.52 (m, 2H, CHMe₂), 1.42 (d, ³J_{HH} = 6.6 Hz, 6H, C(CH₃)Me), 1.24 ppm (d, ³J_{HH} = 6.9 Hz, 6H, CH(CH₃)₂); ¹³C{¹H} NMR (125 MHz, [D₆]DMSO): δ = 156.5 (C-Pd), 122.0, 118.1 (2×C_{im}), 62.3 (CH₂), 51.7 (CHMe₂), 23.8, 21.8 ppm (2×CH(CH₃)₂); elemental analysis calcd (%) for C₁₃H₂₀Cl₂N₄Pd(409.65)-DMSO: C 36.93, H 5.37, N 11.49; found: C 37.16, H 5.11, N 11.56.

Synthesis of 14: Using an identical procedure as for the preparation of **13a**, saturation of a solution of **8b** (40 mg, 0.10 mmol) in MeCN (20 mL) with gaseous Cl₂ for 5 min and subsequent precipitation with Et₂O, gave **14** as an orange solid (38 mg, 48%). Recrystallization from MeOH/DMSO/Et₂O afforded an analytically pure sample. ¹H NMR (500 MHz, [D₆]DMSO): δ = 6.82 (s, 2H, CH₂), 3.77 (s, 6H, NCH₃), 2.89, 2.29 ppm (2×s, 6H, C_{im}-CH₃); ¹³C{¹H} NMR (100 MHz, [D₆]DMSO): δ = 147.0 (C_{im}), 128.4 (C-Cl), 116.0 (C_{im}), 55.0 (CH₂), 33.5 (NCH₃), 11.7, 8.4 ppm (2×C_{im}-CH₃); elemental analysis calcd (%) for C₃₀H₃₂Cl₄N₈O₂Pd₃S₂ (1436.52): C 25.08, H 3.65, N 7.80; found: C 24.82, H 3.80, N 7.57.

Synthesis of 16: By using the same procedure as for the preparation of **13a**, complex **15** (0.15 g, 0.24 mmol) in MeCN (20 mL) was transformed in the presence of Cl₂ to complex **16**, which was isolated as an orange solid (0.10 g, 50%). Recrystallization of **16** from MeOH/DMSO/Et₂O gave an analytically pure sample of [diimidazolium][PdCl₃(DMSO)]₂. ¹H NMR (360 MHz, [D₆]DMSO): δ = 8.36 (s, 2H, H_{im}), 6.66 (s, 2H, CH₂), 4.79 (sept, ³J_{HH} = 6.7 Hz, 2H, CHMe₂), 2.81 (s, 6H, C_{im}-CH₃), 1.52 ppm (d, ³J_{HH} = 6.7 Hz, 12H, CH(CH₃)₂); ¹³C{¹H} NMR (100 MHz, [D₆]DMSO): δ = 142.0, 123.5 (2×C_{im}-C), 111.9 (C_{im}-H), 63.2 (CH₂), 51.5 (CHMe₂), 21.9 (C(CH₃)₂), 10.8 ppm (C_{im}-CH₃); elemental analysis calcd (%) for C₁₉H₃₆Cl₆N₄O₂Pd₂S₂ (842.20): C 27.10, H 4.31, N 6.65; found: C 27.20, H 4.39, N 6.51.

Crystal structure determinations: Suitable single crystals were mounted on a Stoe Mark II-Imaging Plate Diffractometer System (Stoe & Cie, 2002) equipped with a graphite monochromator. Data collection was performed using MoK_α radiation (λ = 0.71073 Å). All structures were solved by direct methods using the program SHELXS-97 and refined by full matrix least squares on F² with SHELXL-97.^[29] All hydrogen atoms were included in calculated positions and treated as riding atoms using SHELXL-97 default parameters. All non-hydrogen atoms were refined anisotropically. For all structures, a semiempirical absorption correction was applied using MULScanABS as implemented in PLATON03.^[30]

Complex **4a** cocrystallized with one molecule of CH₃NO₂, which was strongly disordered over three positions. Therefore, the SQUEEZE option in PLATON was used to calculate the accessible void for the solvent in the unit cell. Nevertheless, the solvent was included for final calculations. Crystals of complex **4b** contained also half a molecule of Et₂O in the asymmetric unit, and complex **8a** cocrystallized with one disordered DMSO molecule. Crystals of complex **8b** also contained one molecule of DMSO in the asymmetric unit, which was disordered over two positions with occupancies of 0.69(1) and 0.31(1), respectively. In addition, the crystal was a twin. The principle HKL file was used. There were approximately 25% overlapped reflections, which were eliminated from the HKL file used. Complex **9** contained one half complex cation, one disordered BF₄[−] ion, and 1.5 disordered DMSO molecules per asymmetric unit. The asymmetric unit of compound **14** contains two organic dications, one [PdCl₄]^{2−} and two [PdCl₃(DMSO)][−] ions, while **16** contains two organic dications, 1.5 [PdCl₄]^{2−} and one [PdCl₃(DMSO)][−] ion, and one water molecule. Details of data collection and refinement parameters are collected in Table 2.

CCDC-717906, CCDC-717907, CCDC-717908, CCDC-717909, CCDC-717910, CCDC-717911, CCDC-717912, CCDC-717913, CCDC-717914 contain the supplementary crystallographic data for this paper. These data can be obtained free of charge from The Cambridge Crystallographic Data Centre via www.ccdc.cam.ac.uk/data_request/cif.

Acknowledgement

We thank F. Fehr and F. Nydegger for technical assistance. This work has been supported by the Swiss National Science Foundation. M. A. gratefully acknowledges an Assistant Professorship from the Alfred Werner Foundation.

- [1] a) D. Bourissou, O. Guerret, F. P. Gabbaï, G. Bertrand, *Chem. Rev.* **2000**, *100*, 39; b) W. A. Herrmann, C. Köcher, *Angew. Chem.* **2002**, *114*, 1342; *Angew. Chem. Int. Ed.* **2002**, *41*, 1290; c) *N-Heterocyclic Carbenes in Synthesis* (Ed.: S. P. Nolan), Wiley-VCH, Weinheim, **2006**; d) F. E. Hahn, M. C. Jahnke, *Angew. Chem.* **2008**, *120*, 3166; *Angew. Chem. Int. Ed.* **2008**, *47*, 3122.
- [2] S. Gründemann, A. Kovacevic, M. Albrecht, J. W. Faller, R. H. Crabtree, *Chem. Commun.* **2001**, 2274.
- [3] a) A. R. Chianese, A. Kovacevic, B. M. Zeglis, J. W. Faller, R. H. Crabtree, *Organometallics* **2004**, *23*, 2461; b) M. Heckenroth, E. Kluser, A. Neels, M. Albrecht, *Angew. Chem.* **2007**, *119*, 6409; *Angew. Chem. Int. Ed.* **2007**, *46*, 6293.
- [4] a) H. Lebel, M. K. Janes, A. B. Charette, S. P. Nolan, *J. Am. Chem. Soc.* **2004**, *126*, 5046; b) M. Viciano, M. Feliz, R. Corberan, J. A. Mata, E. Clot, E. Peris, *Organometallics* **2007**, *26*, 5304; c) L. Yang, A. Krüger, A. Neels, M. Albrecht, *Organometallics* **2008**, *27*, 3161.
- [5] a) S. Sole, H. Gornitzka, W. W. Schoeller, D. Bourissou, G. Bertrand, *Science* **2001**, *292*, 1901; b) V. Lavallo, J. Mafhouz, Y. Canac, B. Donnadieu, W. W. Schoeller, G. Bertrand, *J. Am. Chem. Soc.* **2004**, *126*, 8670; c) V. Lavallo, Y. Ishida, B. Donnadieu, G. Bertrand, *Angew. Chem.* **2006**, *118*, 6804; *Angew. Chem. Int. Ed.* **2006**, *45*, 6652; d) S. Nakafuji, J. Kobayashi, T. Kawashima, *Angew. Chem.* **2008**, *120*, 1157; *Angew. Chem. Int. Ed.* **2008**, *47*, 1141; e) A. Fürstner, M. Alcarazo, K. Radkowski, C. W. Lehmann, *Angew. Chem.* **2008**, *120*, 8426; *Angew. Chem. Int. Ed.* **2008**, *47*, 8302; f) O. Kaufhold, F. E. Hahn, *Angew. Chem.* **2008**, *120*, 4122; *Angew. Chem. Int. Ed.* **2008**, *47*, 4057; for a theoretical discussion, see: g) L. Maron, D. Bourissou, *Organometallics* **2007**, *26*, 1100.
- [6] For examples, see: a) A. Igau, A. Bacciredo, G. Trinquier, G. Bertrand, *Angew. Chem.* **1989**, *101*, 617; *Angew. Chem. Int. Ed. Engl.* **1989**, *28*, 621; b) C. Buron, H. Gornitzka, V. Romanenko, G. Bertrand, *Science* **2000**, *288*, 834; c) P. R. Schreiner, H. P. Reisenauer, F. C. Pickard IV, A. C. Simmonett, W. D. Allen, E. Mátyus, A. G. Császár, *Nature* **2008**, *453*, 906; d) V. Lavallo, C. A. Dyker, B. Donnadieu, G. Bertrand, *Angew. Chem.* **2008**, *120*, 5491; *Angew. Chem. Int. Ed.* **2008**, *47*, 5411. For an excellent discussion, see: e) M. Jones, Jr., R. A. Moss in *Reactive Intermediate Chemistry* (Eds. R. A. Moss, M. S. Platz, M. Jones, Jr.), Wiley, New York, **2004**, pp. 273; f) H. Tomioka in *Reactive Intermediate Chemistry* (Eds. R. A. Moss, M. S. Platz, M. Jones, Jr.), Wiley, New York, **2004**, p. 375.
- [7] For related abnormal carbenes different from 4-imidazolylidenes, see: a) Y. Han, H. V. Huynh, G. K. Tan, *Organometallics* **2007**, *26*, 6581; b) H. G. Raubenheimer, S. J. Cronje, *Dalton Trans.* **2008**, 1265; c) P. Matthew, A. Neels, M. Albrecht, *J. Am. Chem. Soc.* **2008**, *130*, 13534; d) O. Schuster, L. Yang, H. G. Raubenheimer, M. Albrecht, *Chem. Rev.* **2009**, 109DOI: 10.1021/cr8005087.
- [8] M. Albrecht, *Chem. Commun.* **2008**, 3601.
- [9] M. Tafipolsky, W. Scherer, K. Oefele, G. Artus, B. Pedersen, W. A. Herrmann, G. S. McGrady, *J. Am. Chem. Soc.* **2002**, *124*, 5865.
- [10] a) While a zwitterionic ground state may cast doubt on the use of the term “carbene” for these abnormal systems, the isolobal relationship with classical C2-bound NHC ligands warrants a terminological analogy. Similar ambiguities arise when considering the historically grown representation of Fischer and *N*-heterocyclic carbenes^[7d] or for describing cyclic allenes.^[10b,c] For clarity and consistency, the term carbene is therefore preserved. b) M. Christl, B. Engels, *Angew. Chem.* **2009**, *121*, 1566; *Angew. Chem. Int. Ed.* **2009**, *48*, 1538; c) V. Lavallo, C. A. Dyker, B. Donnadieu, G. Bertrand, *Angew. Chem.* **2009**, *121*, 1568; *Angew. Chem. Int. Ed.* **2009**, *48*, 1540.

- [11] a) R. W. Alder, P. R. Allen, S. J. Williams, *J. Chem. Soc. Chem. Commun.* **1995**, 1267; b) Y.-J. Kim, A. Streitwieser, *J. Am. Chem. Soc.* **2002**, *124*, 5757; c) T. L. Amyes, S. T. Diver, J. P. Richard, F. M. Rivas, K. Toth, *J. Am. Chem. Soc.* **2004**, *126*, 4366; d) A. M. Magill, K. J. Cavell, B. F. Yates, *J. Am. Chem. Soc.* **2004**, *126*, 8717; e) A. M. Magill, B. F. Yates, *Aust. J. Chem.* **2004**, *57*, 1205; f) R. Tonner, G. Heydenrych, G. Frenking, *Chem. Asian J.* **2007**, *2*, 1555.
- [12] For examples, where C4 metallation does not affect the C2–H bond, see: a) S. Gründemann, A. Kovacevic, M. Albrecht, J. W. Faller, R. H. Crabtree, *J. Am. Chem. Soc.* **2002**, *124*, 10473; b) L. Campeau, P. Thansandote, K. Fagnou, *Org. Lett.* **2005**, *7*, 1857; c) M. Baya, B. Eguillor, M. A. Esteruelas, M. Olivan, E. Onate, *Organometallics* **2007**, *26*, 6556; d) B. Eguillor, M. A. Esteruelas, M. Olivan, M. Puerta, *Organometallics* **2008**, *27*, 445; e) G. Song, X. Wang, Y. Li, X. Li, *Organometallics* **2008**, *27*, 1187; f) J. Wolf, A. Labande, J.-C. Daran, R. Poli, *Eur. J. Inorg. Chem.* **2008**, 3024. For examples, where C2 to C4 carbene rearrangement was observed, see: g) X. Hu, I. Castro-Rodriguez, K. Meyer, *Organometallics* **2003**, *22*, 3016; h) A. A. Danopoulos, N. Tsoureas, J. A. Wright, M. E. Light, *Organometallics* **2004**, *23*, 166; i) N. Stylianides, A. A. Danopoulos, N. Tsoureas, *J. Organomet. Chem.* **2005**, *690*, 5948; j) C. E. Ellul, M. F. Mahon, O. Saker, M. K. Whittlesey, *Angew. Chem.* **2007**, *119*, 6459; *Angew. Chem. Int. Ed.* **2007**, *46*, 6343; k) M. R. Crittall, C. E. Ellul, M. F. Mahon, O. Saker, M. K. Whittlesey, *Dalton Trans.* **2008**, 4209; l) C. E. Cooke, M. C. Jennings, R. K. Pomeroy, J. A. C. Clyburne, *Organometallics* **2007**, *26*, 6059. For metal-protection of the C2 position, see: m) U. J. Scheele, S. Dechert, F. Meyer, *Chem. Eur. J.* **2008**, *14*, 5112.
- [13] a) P. L. Arnold, S. Pearson, *Coord. Chem. Rev.* **2007**, *251*, 596; b) M. Albrecht, K. J. Cavell, *Organomet. Chem.* **2009**, *35*, 47.
- [14] For exceptions, see ref. [3a] and: a) D. Bacciu, K. J. Cavell, I. A. Fallis, L.-L. Ooi, *Angew. Chem.* **2005**, *117*, 5416; *Angew. Chem. Int. Ed.* **2005**, *44*, 5282; b) M. Alcarazo, S. J. Roseblade, A. R. Cowley, R. Fernandez, J. M. Brown, J. M. Lassaletta, *J. Am. Chem. Soc.* **2005**, *127*, 3290; c) G. Song, Y. Zhang, X. Li, *Organometallics* **2008**, *27*, 1936.
- [15] Only few examples of 2-imidazolylidene complexes with protonated rather than arylated or alkylated nitrogens in *ortho* position: a) C. Y. Liu, D. Y. Chen, G. H. Lee, S. M. Peng, S. T. Liu, *Organometallics* **1996**, *15*, 1055; b) R. Z. Ku, D. Y. Chen, G. H. Lee, S. M. Peng, S. T. Liu, *Angew. Chem.* **1997**, *109*, 2744; *Angew. Chem. Int. Ed. Engl.* **1997**, *36*, 2631; c) X. Wang, H. Chen, X. Li, *Organometallics* **2007**, *26*, 4684; d) M. A. Huertos, J. Perez, L. Riera, A. Menendez-Velazquez, *J. Am. Chem. Soc.* **2008**, *130*, 13530.
- [16] F. H. Allen, O. Kennard, D. G. Watson, L. Brammer, A. G. Orpen, *J. Chem. Soc. Perkin Trans. 2* **1987**, S1.
- [17] Formally, the dicarbene in complex **B** features C5-bound imidazolylidene ligands. In analogy to previous reports on this type of imidazolylidene bonding, we refer to this bonding mode as C4 bonding throughout this manuscript. See also refs. [6d,7,10].
- [18] A D'Sa, L. A. Cohen, *J. Heterocycl. Chem.* **1991**, *28*, 1819.
- [19] a) W. A. Herrmann, C.-P. Reisinger, M. Spiegler, *J. Organomet. Chem.* **1998**, *557*, 93; b) M. Heckenroth, A. Neels, H. Stoeckli-Evans, M. Albrecht, *Inorg. Chim. Acta* **2006**, *359*, 1929.
- [20] a) W. A. Herrmann, J. Schwarz, M. G. Gardiner, *Organometallics* **1999**, *18*, 4082; b) F. E. Hahn, M. Foth, *J. Organomet. Chem.* **1999**, *585*, 241; c) J. Schwarz, V. P. W. Böhm, M. G. Gardiner, M. Grosche, W. A. Herrmann, W. Hieringer, G. Raudaschl-Sieber, *Chem. Eur. J.* **2000**, *6*, 1773; d) S. Ahrens, A. Zeller, M. Taige, T. Strassner, *Organometallics* **2006**, *25*, 5409; e) M. Nonnenmacher, D. Kunz, F. Romminger, T. Oeser, *J. Organomet. Chem.* **2007**, *692*, 2554.
- [21] The insolubility of complexes **8** in less coordinating solvents such as CD₂Cl₂ or CD₃CN has, thus far, precluded the verification of solvent coordination. However, we note that the ¹H chemical shift of one CH₃ group is very similar to that in the bis-solvent complex **12** ($\delta_{\text{H}}=2.21$ ppm). In addition, the two ¹³C NMR signals in **8b** coalesce to a single resonance at $\delta_{\text{C}}=13.1$ ppm when heated to 50 °C in [D₆]DMSO solution.
- [22] M. Heckenroth, E. Kluser, A. Neels, M. Albrecht, *Dalton Trans.* **2008**, 6242.
- [23] See Supporting Information for details.
- [24] For other strongly donating NHC-derived ligand classes, see: a) K. Denk, P. Sirsch, W. A. Herrmann, *J. Organomet. Chem.* **2002**, *649*, 219; b) P. Bazinet, G. P. A. Yap, D. S. Richeson, *J. Am. Chem. Soc.* **2003**, *125*, 13314; c) M. Mayr, K. Wurst, K.-H. Ongania, M. R. Buchmeiser, *Chem. Eur. J.* **2004**, *10*, 1256; d) A. Fürstner, M. Alcarazo, H. Krause, C. W. Lehmann, *J. Am. Chem. Soc.* **2007**, *129*, 12676.
- [25] a) M. Jansen, *Angew. Chem.* **1987**, *99*, 1136; *Angew. Chem. Int. Ed. Engl.* **1987**, *26*, 1098; b) P. Pyykkö, *Chem. Rev.* **1997**, *97*, 597; c) H. Schmidbaur, *Gold Bull.* **2000**, *33*, 3; d) J. J. Vittal, R. J. Puddephatt in *Encyclopedia of Inorganic Chemistry*, 2nd ed. (Ed.: R. B. King), Wiley, New York, **2005**, p. 1673.
- [26] a) K. J. Cavell, D. S. McGuinness, *Coord. Chem. Rev.* **2004**, *248*, 671; b) C. M. Crudden, D. P. Allen, *Coord. Chem. Rev.* **2004**, *248*, 2247; c) D. C. Graham, K. J. Cavell, B. F. Yates, *Dalton Trans.* **2006**, 1768; d) A. M. Magill, B. F. Yates, K. J. Cavell, B. W. Skelton, A. H. White, *Dalton Trans.* **2007**, 3398.
- [27] a) P. Pelagatti in *Handbook of Homogeneous Hydrogenation*, Vol. 1 (Eds.: G. de Vries, C. J. Elsevier), Wiley-VCH, Weinheim, **2007**, p. 71; b) D. S. McGuinness, M. J. Green, K. J. Cavell, B. W. Skelton, A. H. White, *J. Organomet. Chem.* **1998**, *565*, 165; c) D. C. Graham, K. J. Cavell, B. F. Yates, *Dalton Trans.* **2006**, 1768.
- [28] D. S. McGuinness, N. Saendig, B. F. Yates, K. J. Cavell, *J. Am. Chem. Soc.* **2001**, *123*, 4029.
- [29] G. M. Sheldrick, *Acta Crystallogr. Sect. A* **2008**, *64*, 112.
- [30] A. L. Spek, *J. Appl. Crystallogr.* **2003**, *36*, 7.

Received: January 30, 2009
Published online: August 4, 2009